

Electrically tunable lens based on a dual-frequency nematic liquid crystal

Oleg Pishnyak, Susumu Sato, and Oleg D. Lavrentovich

We report on an electrically controlled liquid-crystal-based variable optical lens filled with a dual-frequency nematic material. The lens design employs a hole-patterned electrode structure in a flat nematic cell. In order to decrease the lens switching time we maximize the dielectric torque by using a dual-frequency nematic material that is aligned at an angle approximately 45° with respect to the bounding plates by obliquely deposited SiO_x, and by using an overdrive scheme of electrical switching. Depending on the frequency of the applied field, the director realigns either toward the homeotropic state (perpendicular to the substrates) or toward the planar state (parallel to the substrates), which allows one to control not only the absolute value of the focal length but also its sign. Optical performance of the liquid-crystal lens is close to that of an ideal thin lens. © 2006 Optical Society of America

OCIS codes: 230.3720, 220.3630, 110.2760.

1. Introduction

Optical lenses are widely used in science, industry, and daily life. Development of tunable lenses with variable focal lengths is of great importance for a number of applications, ranging from eyeglasses with an adjustable focal length for vision correction, to fast nonmechanical zooming devices in photocameras and camcorders. One of the actively pursued approaches is based on the effect of reorientation of the nematic liquid crystal (NLC) in the external electric field. The advantage of NLCs is that these materials have a large optical birefringence; as a result, the optical path can be controlled to within a wide range by changing the applied electric field.

The lens effect is achieved when the optical paths of the light beams propagating through different parts of the medium are different. Thus the lens can be formed either by varying the thickness of the material (as in conventional glass lenses) or by varying the

refractive index across the light beam. The development of NLC lenses started in the late 1970s (Refs. 1 and 2) when the design of a NLC cell of varying thickness with conducting electrodes at the curved substrates to control the director orientation was proposed. Subsequent designs used NLC cells of constant thicknesses but with patterned electrodes to achieve nonuniform distributions of the refractive indices by electrical addressing of multiple electrodes,^{3–5} Fresnel-type lenses filled with LCs,^{6–8} LC lenses with spatially varying densities of a polymer network,^{9–11} lenses formed by the patterning of a solid electrode, either slit type^{12,13} or hole type,^{14–16} and other approaches.^{17,18}

One of the fundamental problems in the development of electrically controlled NLC lenses is their slow response. The NLC lens needs to be relatively thick for the sufficiently wide range of focus changes. However, by increasing the thickness d of the lens, one significantly increases the time needed for director reorientation, as the latter scales¹⁹ as d^2 . The typical estimate of the director reorientation time is the quantity¹⁹ $\tau_{\text{off}} = \gamma_1 d^2 / \pi^2 K$, where γ_1 and K are the characteristic rotational viscosity and elastic constant of NLC, respectively; τ_{off} describes how fast the director relaxes into the original state controlled by the surface alignment in the cell when the field is switched off. For example, a cell of thickness $d = 100 \mu\text{m}$ filled with a typical NLC material with¹⁹ $K = 10^{-11} \text{ N}$, $\gamma_1 \approx 0.1 \text{ kg m}^{-1} \text{ s}^{-1}$ needs approximately $\tau_{\text{off}} \approx 10 \text{ s}$ to relax the director when the field is

O. Pishnyak (opp@lci.kent.edu) and O. D. Lavrentovich (odl@lci.kent.edu) are with the Chemical Physics Interdisciplinary Program, Kent State University, P.O. Box 5190, Kent, Ohio 44242-0001. O. D. Lavrentovich is also with the Liquid Crystal Institute, Kent State University, P. O. Box 5190, Kent, Ohio 44242-0001. S. Sato is with the Department of Electrical and Electronic Engineering, Akita University, 1-1 Tegata Gakuen-machi, Akita-shi, 010-8502 Japan.

Received 26 September 2005; revised 21 December 2005; accepted 23 December 2005; posted 4 January 2006 (Doc. ID 64997).

0003-6935/06/194576-07\$15.00/0

© 2006 Optical Society of America

switched off. The switch-on state can be estimated as

$$\tau_{\text{on}} = \frac{\gamma_1 d^2}{\pi^2 K} \left(\frac{U_c^2}{U^2 - U_c^2} \right),$$

where U_c is the typical threshold voltage of director reorientation. Therefore τ_{on} can be reduced by applying an electric field of large amplitude; however, the same principle cannot be applied to reduce τ_{off} . The problem has been addressed in the past by using thinner cells or polymer-stabilized NLC.^{9–11} Thinner cells, however, result in a reduced optical power of the lens, while adding the polymer component might cause light scattering.

Here we propose an approach based on the so-called dual-frequency NLC, i.e., the NLC in which the sign of dielectric anisotropy $\Delta\epsilon$ changes from positive to negative when the frequency of the applied field increases.¹⁹ The latter feature allows one to switch the director in both directions, parallel and perpendicular to the field, by applying the electric field of low and high frequencies. The most important distinctive feature of our approach is that the nematic director is aligned at the angle approximately 45° with respect to the bounding plates²⁰ and not tangentially to it, as in Ref. 8. As a result, the angle β between the director and the direction of the field is close to 45° , which allows us to maximize the reorienting dielectric torque that is proportional to $\sin 2\beta$. In addition, the director reorientation in both directions is accelerated by elevated amplitudes of the applied voltage (an overdriving scheme). As a result, we have reduced the switching time of a cell with thickness $110\ \mu\text{m}$ down to at least $400\ \text{ms}$, which is approximately 1 order of magnitude faster than in a regular design.

The lens is based on a flat NLC cell with a hole-patterned electrode. Application of the electric field results in a nonuniform director configuration and thus a varying effective index of refraction in the plane of the cell that leads to the lens effect. A high-pretilt alignment and the dual-frequency properties of the NLC allow us to realize both converging and diverging lenses in the same cell. Note that dual-frequency NLCs have been used previously as switchable fillers in Fresnel lenses with varying thickness of the cell⁸; however, the concrete thickness of the nematic slab has not been indicated, and thus it is difficult to make a quantitative comparison of the flat cell lens versus Fresnel lens approach.

Finally, we propose a double-lens design to control the focal shift with respect to the lens axis.

2. Experiment

A. Design of the Liquid-Crystal-Based Lens

We construct the dual-frequency NLC lens from two different glass plates. One plate is $1.1\ \text{mm}$ thick with a continuous transparent indium tin oxide (ITO) electrode. The second substrate is $0.2\ \text{mm}$ thick with a hole-patterned aluminum electrode (Fig. 1). To ensure the optimum lens properties, the ratio of the lens

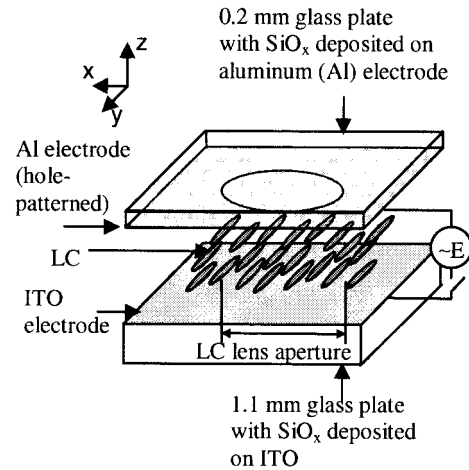


Fig. 1. Design of the dual-frequency nematic lens.

diameter D to the lens thickness d should be²¹ between 2 and 3. In our case the lens aperture, i.e., the diameter of the hole, is $D = 300\ \mu\text{m}$ while $d = 110\ \mu\text{m}$. The cell is filled with the dual-frequency NLC material MLC-2048 (Merck), which has the positive sign of dielectric anisotropy $\Delta\epsilon = \epsilon_{||} - \epsilon_{\perp} > 0$ for frequencies f of the applied electric field smaller than the crossover frequency $f_c = 12\ \text{kHz}$ (at 20°C) and negative $\Delta\epsilon < 0$ when $f > f_c$. Here $\epsilon_{||}$ and ϵ_{\perp} are the dielectric permittivities of the NLC in the directions parallel and perpendicular to the LC director, respectively. When $\Delta\epsilon > 0$, the director reorients toward the electric field; when $\Delta\epsilon < 0$, it reorients perpendicularly to the field. We used two characteristic driving frequencies, $f = 1\ \text{kHz}$, at which $\Delta\epsilon = 3.2$, and $f = 50\ \text{kHz}$, at which $\Delta\epsilon = -3.1$ (both values of the dielectric anisotropy correspond to the temperature 20°C). The optical birefringence of the material $\Delta n = 0.22$ at $\lambda = 589\ \text{nm}$. The initial orientation of the director is set at approximately 45° with respect to the bounding plates by treating the substrates with an obliquely deposited layer of SiO_x . Though a high-pretilt alignment of the LC director leads to a phase loss in comparison with the planar (low-pretilt) geometry, a high-pretilt angle plays the key role in realizing both positive and negative lenses in the same cell through the change of the frequency of the applied field. In addition, the 45° pretilt maximizes the reorienting torque of the electric field. The hole-patterned electrode provides a nonlinear distribution of the electric field inside the LC layer, which causes a nonuniform reorientation of the LC director and thus the lens effect.^{14,21} For example, in Figs. 1 and 2 (below) light beams linearly polarized along the x axis and propagating through different regions of the lens would experience a different optical path $n_{\text{eff}}d$, where

$$n_{\text{eff}} = \frac{n_o n_e}{(n_o^2 \cos^2 \theta + n_e^2 \sin^2 \theta)^{1/2}}$$

is the local field-dependent effective refractive index of the LC, θ is the local field-dependent angle between

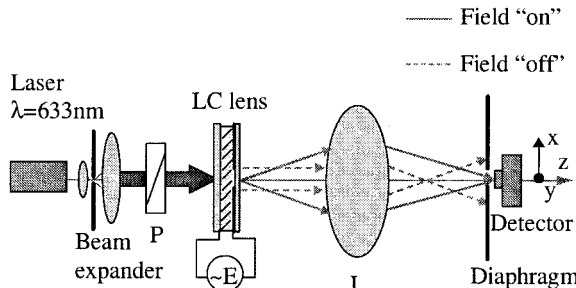


Fig. 2. Experimental setup for response time measurements.

the direction of light polarization and the LC director, and n_o and n_e are the ordinary and the extraordinary LC refractive indices, respectively.

B. Response Times

The experimental setup for the response time measurements is shown in Fig. 2. A light beam from a He–Ne laser ($\lambda = 633$ nm) passes through a beam expander and a polarizer P oriented parallel to the projection of the LC easy axis onto the xy plane (Fig. 2), then hits the LC lens and focuses by the glass lens L into an optical detector connected to an oscilloscope (TDS 210, Tektronix). If there is no electric field, the diaphragm in front of the detector cuts a significant part of the laser beam and the optical signal is minimal (the diaphragm aperture is 250 μm). If the electric field is applied at 1 kHz, then a converging LC lens is induced and the light beam passes through the diaphragm causing an increase in the light intensity measured by the detector. In Fig. 3(a) we show the optical response of the designed lens (top trace) under the applied electrical signal (bottom trace). The applied electric field is a sequence of high-amplitude special short pulses (SSP) accelerating the initial stage of director reorientation and low-amplitude holding pulses at two frequencies (1 and 50 kHz).²⁰ The dynamics of the lens response is composed of fast and slow components. Initially, the lens shows a fast response time of approximately 50 ms during the transition to the focusing state [Fig. 3(b)], but then the optical signal experiences a slow drift over approximately 400 ms, during which the optical signal changes by approximately 10–15%. The reason for this drift might be a backflow effect and dielectric heating.²² The same phenomenon occurs when the lens relaxes back to the nonfocusing state [Fig. 3(c)]: a fast reorientation during 75 ms is followed by a slow drift of approximately 400 ms.

C. Lens Optical Performance

We now discuss the optical characteristics of the designed LC lens and compare its performance with an ideal thin lens.

We placed the LC lens between two crossed polarizers in such a way that the projection of the LC easy axis on the xy plane is at 45° to both polarizer axes. By using a movable CCD camera with an objective we can monitor the output aperture plane of the lens as

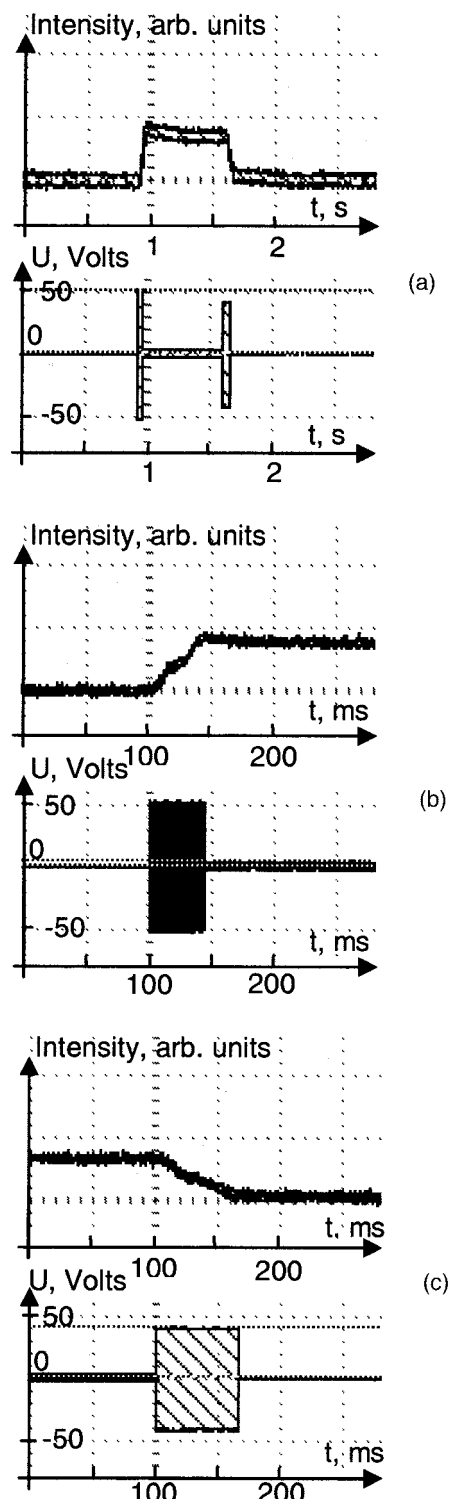


Fig. 3. Response time of the 110 μm thick lens. (a) Lens optical response (top trace) under applied voltage (bottom trace). The driving signal (bottom trace) is a sequence of SSP (50 V rms, 1 kHz) followed by a holding voltage (4 V rms, 1 kHz) followed by SSP of 40 V rms at 50 kHz. (b) Transition to the focusing state (top trace). Electric signal applied (bottom trace) is a sequence of SSP (50 V rms) followed by a holding voltage (4 V rms) at 1 kHz. (c) Relaxation from the focusing state to the uniform (nonfocusing) director state (top trace). The transition is triggered by SSP of 40 V rms at 50 kHz (bottom trace).

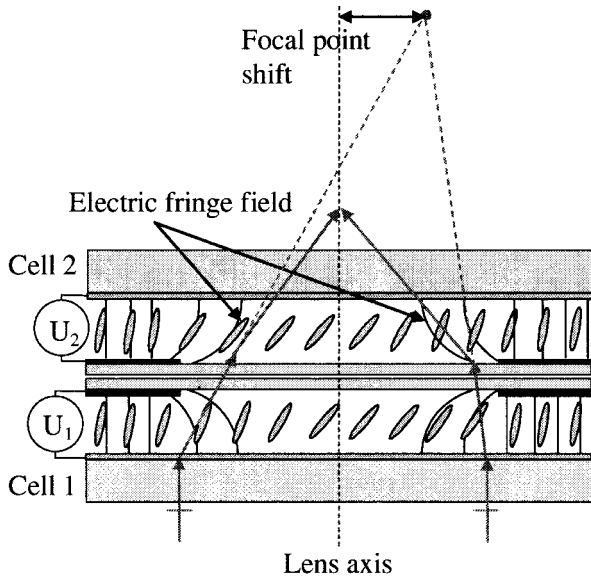


Fig. 4. Double lens design. Two hole-patterned NLC lenses are coaxial and oriented in a “head-to-head” fashion. The simplified ray paths and director distribution are shown for the field applied at 1 kHz. Lines of the electric fringe field are shown by thin curves. The off-axis focusing of the light caused by the first lens is corrected by the second lens.

well as its focal plane. The experimental setup is similar to that shown in Fig. 2 except that now we placed the lens between two crossed polarizers. If the electric field is applied, we can observe the appearance of interference fringes in the output aperture plane of the lens caused by the phase shift between the ordinary and the extraordinary light waves. The number of fringes indicates the optical power of the lens. When the applied voltage increases, the number of fringes and the lens optical power increase too. Due to the dual-frequency properties of the nematic material and a high-pretilt alignment, we can realize both positive and negative lens regimes by applying the electrical field with frequencies of 1 and 50 kHz, respectively. In a cell with a nonzero surface pretilt, the angle between the electric fringe field and the LC director is different²³ at the antipodal points of the hole-patterned electrode (Fig. 4). As a result, the pattern of the field-induced director reorientation and effective refractive index across the hole region is nonsymmetrical; the interference pattern shifts with respect to the lens axis. In order to correct the off-axis focusing, we propose the double lens design shown in Fig. 4. Two identical hole-patterned lenses are coaxial and assembled in a head-to-head fashion. The symmetry of this configuration is such that the difference between the direction of the fringe field and the easy axes of two lenses are mutually compensated. In Fig. 5 we show that by adjusting voltages U_1 and U_2 applied to cells 1 and 2 we can correct the off-axis focusing of the single lens. If $U_1 = 0$ the interference fringes observed at the output aperture plane of the system are off center (Fig. 5, top row), and the lens focal point is shifted away from the lens

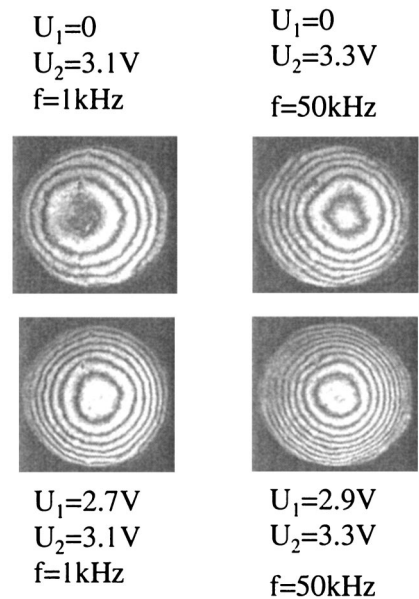


Fig. 5. Output aperture plane of the double lens illustrating the correction of the off-axis focusing effect based on application of the electric field to both cells. The left and right parts of the picture illustrate positive and negative lenses, respectively. Top row: $U_1 = 0$, interference fringes are not centered; Bottom row: the electric field is applied to both lenses at 1 and 50 kHz; the interference fringes are centered; the lens focal point is located on the lens axis.

axis. After adjusting U_1 , the interference fringes become well centered (Fig. 5, bottom row), so the focal point shift is corrected. The results of correction are shown for both frequencies applied. The focal point shift can be used as a desirable feature in beam deflecting devices. Note that the optical power of a double lens system is larger as compared to a single lens. When $U_1 \neq 0$, the number of interference fringes and lens optical power increase (Fig. 5, bottom row).

As the thickness of the designed NLC lens is $110\text{ }\mu\text{m}$ and the focal length is of the order of millimeters, we can neglect the displacement of the light beam inside the LC layer. In this case the NLC lens can be considered as a thin lens introducing a phase shift to the incident wave. The optical field of a plane wave A_L behind the thin lens is described by²⁴

$$A_L(x, y) = \exp[iknd] \exp\left[-i \frac{k}{2f_L} (x^2 + y^2)\right], \quad (1)$$

where $k = 2\pi/\lambda$ is the wavenumber (λ is the wavelength), and n , d , and f_L are the lens refractive index, thickness, and focal length, respectively. The first exponent describes a constant phase shift, ϕ_0 , introduced by a thin lens, while the second exponent is a quadratic approximation of a spherical wave. Thus the phase retardation ϕ of the NLC lens along the x axis (direction of the initial easy axis projection on the plane of the cell) can be written as follows:

$$\phi = \phi_0 - \frac{2\pi}{\lambda} \frac{1}{2f_L} x^2. \quad (2)$$

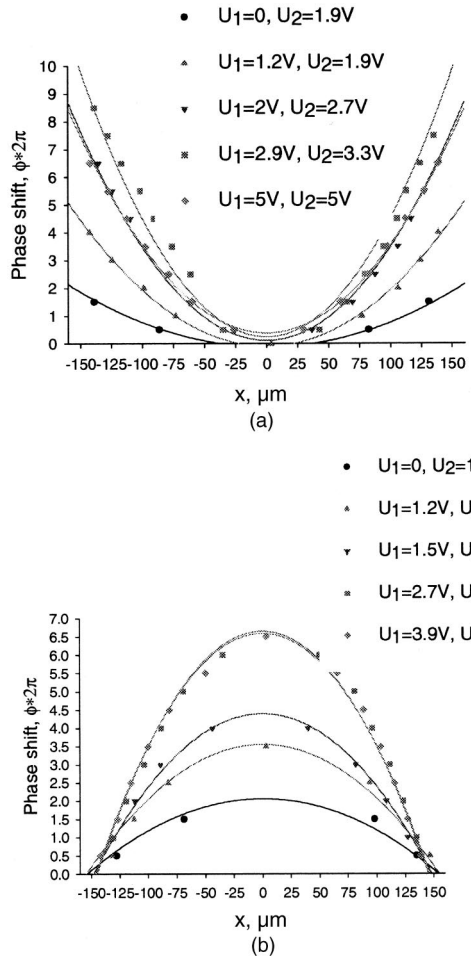


Fig. 6. Phase retardation measurements (dots) of the double NLC lens and the quadratic fitting curves (the solid curves) at two frequencies of the applied electric field: (a) 50 kHz and (b) 1 kHz.

The phase retardation of LC lenses at different voltages can be found from the number of interference fringes appearing at the lens output aperture. The distance between two neighboring dark (or white) fringes corresponds to the phase retardation of 2π . In Fig. 6 we show the experimental results of phase retardation measurements (dots) of the double lens together with the fitting curves (the solid curves) at two frequencies of the applied electric field. The fitting curves were obtained from Eq. (2) with the focal length f_L as a fitting parameter. The fitting curves are very close to the experimental data; it means that for each voltage applied, the induced NLC lens behaves similar to a thin lens with a certain focal length. Deviation of the experimental data from the curves describing the behavior of an ideal thin lens indicates the presence of aberrations in the system, such as coma and astigmatism. The aberrations are most probably caused by a nonsymmetrical distribution of the refractive index with respect to the geometric axis of the system. In Fig. 7 we show the focal length dependence of the double NLC lens versus the applied voltage. Focal length values were extracted from the results of the quadratic fitting. We verified

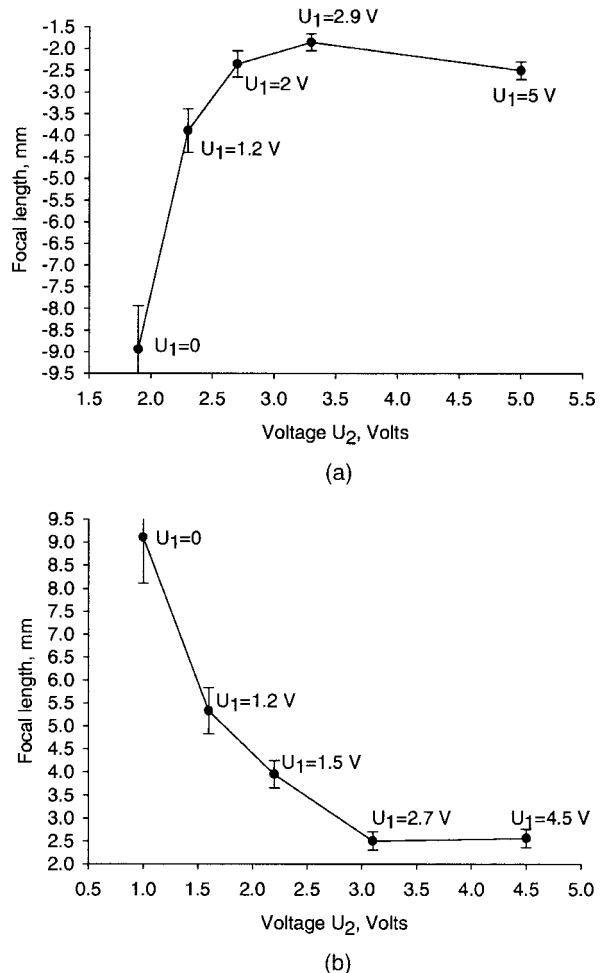


Fig. 7. Focal length of the double LC lens versus the applied voltage at two frequencies: (a) 50 kHz and (b) 1 kHz.

them independently by moving the CCD camera along the z axis. The obtained results confirm that both negative and positive lenses for the very same nematic cell can be realized by choosing the frequency of the applied voltage at either 50 or 1 kHz. The focal length varies from $-\infty$ to -1.9 mm (the optical power varies from 0 to -520 diopters) at 50 kHz, and from $+\infty$ to $+2.5$ mm (the optical power varies from 0 to $+400$ diopters) at 1 kHz. As the applied voltage increases, the lens focal length decreases (Fig. 7) but at some critical voltage due to the electric fringing field effect and elastic properties of the LC, the director in the central part of the lens starts to reorient too, and the optical retardation and focal length of the lens both saturate. As the voltage increases further, the NLC lens becomes distorted.

3. Discussion

Let us discuss the advantages of the proposed NLC lens design. First, the dielectric torque τ acting on the nematic director is proportional to $\sin 2\beta$, where β is an angle between the electric field and nematic director. A combination of the overdrive scheme with a high-pretilt angle ($\beta \approx 45^\circ$) results in strong restor-

ing torques that facilitate director reorientation from the 45° tilted state toward both homeotropic and planar states,²⁰ which in turn reduces the response time during focus change down to at least 400 ms for the 110 μm thick cell. It is more than 1 order of magnitude faster than in regular cell designs with $\tau_{\text{off}} = 10$ s.

Second, a tilt of the LC molecules eliminates the threshold of reorientation allowing continuous tuning of the optical power of the double LC lens from -520 to +400 diopters in the same cell as illustrated in the example above with $\lambda = 633$ nm.

Third, a high-pretilt alignment of the LC molecules allows us to avoid the appearance of disclination lines that may cause light scattering and slow relaxation during lens switching. While in planar cells one needs to apply an in-plane electric field in order to force the molecules to rotate in the same direction to eliminate the disclinations,²³ in our approach no additional field is required; the problem of disclination line appearance is solved by the high-pretilt alignment of LC molecules.

By varying the voltage applied to both cells in the double lens approach, we can focus the light not only along the lens axis, but also move the focus along a 3D trajectory or in the xy plane, which was realized earlier for planar cells through the application of the in-plane field.¹⁶ This feature may be used in beam deflecting devices.

Note that the actual response time is determined by a fast component of the order of 50–100 ms with a subsequent slow drift of approximately 400 ms for the 110 μm cell. The slow relaxation [Fig. 3(a)] is most probably caused by material flow and dielectric heating. Slow drift of the optical signal can be reduced by either polymer stabilization or using the thinner cells (of course, in the latter case the LC lens will be less powerful).

The proposed lens design is polarization dependent, which means that only light with polarization parallel to the easy axis will be focused, while the light with orthogonal polarization will remain unfocused. If necessary, the polarization dependency can be eliminated by stacking LC cells with the easy axes oriented perpendicularly to each other.²⁵ Note that in our experiments, we used cells with a relatively small aperture of 0.3 mm. For applications in photocameras and camcorders, the LC lenses should be few times larger. The techniques to upscale the LC lenses to the 1–5 mm range aperture have been described, for example, in Ref. 15. These techniques are applicable to the dual-frequency design proposed in this work.

4. Conclusions

We have demonstrated a NLC-based lens with a hole-patterned electrode structure, the focal length of which can be tuned by the electric field. A combination of a high-pretilt alignment, dual-frequency properties of the nematic material, and an overdrive scheme allows us to reduce the response time during focus change from approximately 10 s down to 0.4 s

for a 110 μm thick cell; most of the director structure is switched to within the first 50–100 ms. The proposed design allows one to use the same cell as either a negative or positive lens by changing the frequency of the applied field. The optical characteristics of the system are close to the performance of an ideal thin lens but some wavefront aberrations are still present. The optical power of the system with the aperture $D = 300 \mu\text{m}$ can be continuously tuned from -520 to +400 diopters ($\lambda = 633$ nm) in the double NLC lens approach. Such a design can be used to achieve fast optical communication between multiple channels, in microlens arrays,^{26–29} in beam steering or scanning devices, or for fast nonmechanical zooming in miniature cameras, for example. In the latter case isotropic fluids have been recently proposed as the focusing medium.^{30,31} Isotropic liquid lenses are based on the electrowetting effect, which allows one to control the droplet or the meniscus shape by applying an electric field. If the densities of two liquids in contact are equal, the meniscus is rather insensitive to the external vibrations and shocks.³¹ The advantage of the NLC lenses is in a greater mechanical stability against vibrations as the nematic fluid is confined between two rigid plates, and the refractive changes are caused by molecular reorientation, not by the variation of the fluid surface or interface.

We thank Andrii Golovin, Marenori Kawamura, Tomoyuki Sakamoto, Sergij Shiyanskii, and Mao Ye for their help and valuable discussions. This research was partially supported by the National Science Foundation and the Japan Society for the Promotion of Science.

References

1. C. Bricot, M. Hareng, and E. Spitz, "Optical projection device and an optical reader incorporating this device," U.S. patent 4,037,929 (26 July 1977).
2. S. Sato, "Liquid-crystal lens-cells with variable focal length," *Jpn. J. Appl. Phys.* **18**, 1679–1684 (1979).
3. S. T. Kowal, D. S. Cleverly, and P. G. Kornreich, "Focusing by electrical modulation of refraction in a liquid crystal cell," *Appl. Opt.* **23**, 278–289 (1984).
4. N. A. Riza and M. C. DeJule, "Three-terminal adaptive nematic liquid-crystal lens device," *Opt. Lett.* **19**, 1013–1015 (1994).
5. W. W. Chan and S. T. Kowal, "Imaging performance of the liquid-crystal-adaptive lens with conductive ladder meshing," *Appl. Opt.* **36**, 8958–8969 (1997).
6. S. Sato, A. Sugiyama, and R. Sato, "Variable-focus liquid-crystal Fresnel lens," *Jpn. J. Appl. Phys. Part 2* **24**, L626–L628 (1985).
7. S. Sato, T. Nose, R. Yamaguchi, and S. Yanase, "Relationship between lens properties and director orientation in a liquid crystal lens," *Liq. Cryst.* **5**, 1435–1442 (1989).
8. S. Suyama, M. Date, and H. Takada, "Three-dimensional display system with dual-frequency liquid-crystal varifocal lens," *Jpn. J. Appl. Phys. Part 1* **39**, 480–484 (2000).
9. H. Ren and S.-T. Wu, "Tunable electronic lens using a gradient polymer network liquid crystal," *Appl. Phys. Lett.* **82**, 22–24 (2003).
10. Y.-H. Fan, H. Ren, and S.-T. Wu, "Switchable Fresnel lens using polymer-stabilized liquid crystals," *Opt. Express* **11**, 3080–3086 (2003).

11. V. Presnyakov and T. Galstian, "Polymer stabilized liquid crystal lens for electro-optical zoom," in *Photonics North 2004: Optical Components and Devices*, J. C. Armitage, S. Fafard, R. A. Lessard, G. A. Lampropoulos, eds., Proc. SPIE **5577**, 861–869 (2004).
12. Z. He, T. Nose, and S. Sato, "Optical performance of liquid crystal cells with asymmetric slit-patterned electrodes in various applied field configurations," *Jpn. J. Appl. Phys. Part 1* **33**, 1091–1095 (1994).
13. H. Ren, Y.-H. Fan, S. Gauza, and S.-T. Wu, "Tunable-focus cylindrical liquid crystal lens," *Jpn. J. Appl. Phys. Part 1* **43**, 652–653 (2004).
14. T. Nose and S. Sato, "A liquid crystal microlens obtained with a nonuniform electric field," *Liq. Cryst.* **5**, 1425–1433 (1989).
15. M. Ye and S. Sato, "Optical properties of liquid crystal lens of any size," *Jpn. J. Appl. Phys. Part 2* **41**, L571–L573 (2002).
16. M. Ye and S. Sato, "Liquid crystal lens with focus movable along and off axis," *Opt. Commun.* **225**, 277–280 (2003).
17. A. F. Naumov, M. Yu. Loktev, I. R. Guralnik, and G. Vdovin, "Liquid-crystal adaptive lenses with modal control," *Opt. Lett.* **23**, 992–994 (1998).
18. I. R. Gural'nik and S. A. Samagin, "Optically controlled spherical liquid-crystal lens: theory and experiment," *Quantum Electron.* **33**, 430–424 (2003).
19. L. M. Blinov and V. G. Chigrinov, *Electrooptic Effects in Liquid Crystal Materials* (Springer, 1994).
20. A. B. Golovin, S. V. Shiyanskii, and O. D. Lavrentovich, "Fast switching dual-frequency liquid crystal optical retarder, driven by an amplitude and frequency modulated voltage," *Appl. Phys. Lett.* **83**, 3864–3866 (2003).
21. S. Sato, "Applications of liquid crystals to variable-focusing lenses," *Opt. Rev.* **6**, 471–485 (1999).
22. Y. Yin, M. Gu, A. B. Golovin, S. V. Shiyanskii, and O. D. Lavrentovich, "Fast switching optical modulator based on dual frequency nematic cell," *Mol. Cryst. Liq. Cryst.* **421**, 133–144 (2004).
23. M. Ye, B. Wang, and S. Sato, "Driving of liquid crystal lens without disclination occurring by applying in-plane electric field," *Jpn. J. Appl. Phys. Part 1* **42**, 5086–5089 (2003).
24. J. W. Goodman, *Introduction to Fourier Optics* (McGraw-Hill, 1968).
25. M. Ye and S. Sato, "Liquid crystal lens with insulator layers for focusing light waves of arbitrary polarizations," *Jpn. J. Appl. Phys. Part 1* **42**, 6439–6440 (2003).
26. L. G. Commander, S. E. Day, and D. R. Selviah, "Variable focal length microlenses," *Opt. Commun.* **177**, 157–170 (2000).
27. M. Ye, S. Hayasaka, and S. Sato, "Liquid crystal lens array with hexagonal-hole-patterned electrodes," *Jpn. J. Appl. Phys. Part 1* **43**, 6108–6111 (2004).
28. H. Ren, Y.-H. Fan, Y.-H. Lin, and S.-T. Wu, "Tunable-focus microlens arrays using nanosized polymer-dispersed liquid crystal droplets," *Opt. Commun.* **247**, 101–106 (2005).
29. H. Ren, J. R. Wu, Y.-H. Fan, Y.-H. Lin, and S.-T. Wu, "Hermaphroditic liquid-crystal microlens," *Opt. Lett.* **30**, 376–378 (2005).
30. T. Krupenkin, S. Yang, and P. Mach, "Tunable liquid micro-lens," *Appl. Phys. Lett.* **82**, 316–318 (2003).
31. S. Kuiper and B. H. W. Hendriks, "Variable-focus liquid lens for miniature cameras," *Appl. Phys. Lett.* **85**, 1128–1130 (2004).